Proc. Natl. Acad. Sci. USA
Vol. 96, pp. 2333–2338, March 1999
Medical Sciences

Imaging adenoviral-directed reporter gene expression in living animals with positron emission tomography

SANJIV S. GAMBHIR*†‡§¶‖, JORGE R. BARRIO†‡, MICHAEL E. PHELPS*†‡§, MEERA IYER*†, MOHAMMAD NAMAVARI†‡, NAGICHETTIAR SATYAMURTHY†‡, LILY WU¶**, LEETA A. GREEN*§, EILEEN BAUER*, DUNCAN C. MACLAREN*,**, KHOI NGUYEN*, ARNOLD J. BERK¶**, SIMON R. CHERRY*†‡, AND HARVEY R. HERSCHMAN*†‡¶**

*The Crump Institute for Biological Imaging, †University of California/Department of Energy Laboratory of Structural Biology and Molecular Medicine, ‡Department of Molecular and Medical Pharmacology, The Division of Nuclear Medicine, **Molecular Biology Institute, §Department of Biomathematics, and ¶University of California–Jonsson Comprehensive Cancer Center, University of California School of Medicine, Los Angeles, CA 90095-1770

Communicated by David S. Eisenberg, University of California, Los Angeles, CA, December 30, 1998 (received for review October 23, 1998)

ABSTRACT **We are developing quantitative assays to repeatedly and noninvasively image expression of reporter genes in living animals, using positron emission tomography (PET). We synthesized positron-emitting 8-[18F]fluoroganciclovir (FGCV) and demonstrated that this compound is a substrate for the herpes simplex virus 1 thymidine kinase enzyme (HSV1-TK). Using positron-emitting FGCV as a PET reporter probe, we imaged adenovirus-directed hepatic expression of the HSV1-tk reporter gene in living mice. There is a significant positive correlation between the percent injected dose of FGCV retained per gram of liver and the levels of hepatic HSV1-tk reporter gene expression ($r^2 > 0.80$). Over a similar range of HSV1-tk expression *in vivo*, the percent injected dose retained per gram of liver was 0–23% for ganciclovir and 0–3% for FGCV. Repeated, noninvasive, and quantitative imaging of PET reporter gene expression should be a valuable tool for studies of human gene therapy, of organ/cell transplantation, and of both environmental and behavioral modulation of gene expression in transgenic mice.**

Most methods to image gene expression from transplanted "reporter" genes in rodents, primates, and humans require the use of fixed tissue, obtained either from biopsies or after death. Newer methods using luciferase (1) and green fluorescent protein (2) as reporter genes are limited in their *in vivo* application to transparent organisms. Positron emission tomography (PET) utilizes molecules labeled with positron-emitting radioisotopes, in trace quantities, to observe and measure rates of biochemical processes in tissues of living subjects (3, 4). Typically, either positron-labeled substrates for intracellular enzymes or positron-labeled ligands for cellular receptors are used as PET probes. Retention of the PET probe in target tissues, as a result either of (*i*) conversion of a positron-labeled enzyme substrate to a "trapped" metabolic product or (*ii*) binding of a positron-labeled ligand to its receptor, is detected and quantitatively imaged in living subjects with the tomograph. A review of the principles involved in developing assays for imaging reporter gene expression can be found elsewhere (5, 6). To noninvasively image small animals such as mice we recently have developed microPET technology (7), which has a volumetric resolution of approximately 8 mm^3. MicroPET facilitates development of PET reporter gene assays by permitting their validation in murine models.

The herpes simplex virus 1 thymidine kinase reporter gene (HSV1-tk) has been explored by several groups for the purposes of imaging reporter gene expression (8–15). HSV1-TK enzyme has relaxed substrate specificity as compared with mammalian thymidine kinases and can phosphorylate acycloguanosine and uracil derivatives (16, 17). FIAU [5-iodo-2′-fluoro-2′-deoxy-1-β-D-arabinofuranosyl-5′-iodouracil] labeled with carbon-14, iodine-131, and iodine-124 (8, 9, 18), 8-[18F]fluoroganciclovir (FGCV) (19–21), and 9-[(3-[18F]fluoro-1-hydroxy-2-propoxy)methyl]guanine (11, 13) all have been investigated preliminarily as reporter probes to image HSV1-tk. We demonstrated previously the feasibility of using carbon-14-labeled ganciclovir to monitor adenoviral-mediated delivery of HSV1-tk reporter gene expression in mice, using digital whole-body autoradiography (DWBA) (15). We now have developed a quantitative imaging assay, using FGCV as a PET reporter probe, to repeatedly image the expression of the HSV1-tk PET reporter gene in living animals by taking advantage of the short half-life (110 min) for fluorine-18.

MATERIALS AND METHODS

Radiolabeled Compounds. 8-[^{3}H]Ganciclovir (8-[^{3}H]GCV) (13.1 Ci/mmol) was obtained from Moravek Biochemicals (La Brea, CA). Radiochemical purity, determined by HPLC, was greater than 97%. FGCV was synthesized as described previously (19, 20) at a specific activity of 2–5 Ci/mmol. Radiochemical purity of FGCV exceeded 99%, as determined by HPLC.

HPLC Analysis. 8-[^{3}H]GCV and FGCV and their metabolites from cell/tissue extracts were analyzed by using HPLC with a Whatman Partisil 10 SAX column. The column was eluted with a linear KH_2PO_4 gradient, 0.01–1.0 M (pH 3.7, at a flow rate of 1 ml/min), and monitored with a UV detector, with wavelength set at 254 nm. Radioactive fractions were collected in samples taken over 1–2 min.

Radioactivity Determinations. All tritium analyses were performed with a Beckman LS-9000 Liquid Scintillation Counter with Biosafe II (Research Products International) scintillation fluid. Corrections for background activity and efficiency (51.4%) based on calibrated standards (Beckman Coulter) also were performed to obtain dpm. Tritium counts also were corrected for quenching effects. All fluorine-18 analyses were performed in either a dose calibrator (Capintec CRC-5R, Ramsey, NJ) or a well counter (T_m Analytic, Tampa, FL), correcting for efficiency differences between these two systems.

Construction and Purification of Adenoviruses. Construction, purification, and characterization of an adenovirus in

The publication costs of this article were defrayed in part by page charge payment. This article must therefore be hereby marked "*advertisement*" in accordance with 18 U.S.C. §1734 solely to indicate this fact.

PNAS is available online at www.pnas.org.

Abbreviations: HSV1-tk, herpes simplex virus 1 thymidine kinase gene; HSV1-TK, HSV1 thymidine kinase enzyme; DWBA, digital whole-body autoradiography; FGCV, 8-[18F]fluoroganciclovir; CMV, cytomegalovirus; ROI, regions of interest; pfu, plaque-forming unit.

‖To whom reprint requests should be addressed at: University of California School of Medicine, 700 Westwood Plaza, A-222B CIBI, Los Angeles, CA 90095-1770. e-mail: sgambhir@mednet.ucla.edu.

which HSV1-tk is expressed from a cytomegalovirus (CMV) promoter (AdCMV-HSV1-tk) and a control virus that is an E1-deletion mutant have been described previously (15).

Cell Lines, Culture Conditions, and Transfection Procedures. C6 rat glioma cells (used as a control cell line) and the C6 HSV1-tk stable transfectant (C6-stb-tk+) were provided by M. Black (Chiroscience R & D, Bothell, WA). Cells used for 8-[^{3}H]GCV and FGCV uptake studies were grown in 12-well plates in DMEM supplemented with 5% FBS/1% penicillin-streptomycin/1% L-glutamine.

For adenovirus transfection studies, C6 cells were grown as monolayers in t75 flasks. Twenty-four hours after plating, varying concentrations of AdCMV-HSV1-tk virus (to produce C6 tk+ cells) or control virus (to produce C6 tk− cells) were added to separate flasks. Cells were exposed to adenovirus (27 h) and then replated and cultured for an additional 22 h in 12-well plates (for tracer uptake studies) or 100-mm dishes (for assay of HSV1-TK enzyme and mRNA levels).

HSV1-TK Mediated Phosphorylation of Ganciclovir and FGCV. Ganciclovir (Parke-Davis) (0.07 mg/ml) was incubated at 37°C with 50 ng HSV1-TK (provided courtesy of M. Black) in the presence of TK buffer (1 mM DTT/5 mM ATP/5 mM $MgCl_2$/25 mM NaF/40 mM KCl/0.5 mg/ml BSA/20 mM K-phosphate buffer, pH 7.6) for 20 and 40 min. The same method was used for FGCV, except that the concentration of FGCV was 0.5 mg/ml and the incubation times were 60 and 120 min. A 25-μl sample of the incubation mixture was analyzed by HPLC.

Dephosphorylation of Monophosphate Products. Buffer (2.5 μl; 10 mM $ZnCl_2$/10 mM $MgCl_2$/100 mM Tris·Cl, pH 8.3) and 1 unit *Escherichia coli* alkaline phosphatase (Sigma) were added to 15 μl supernatant obtained from incubation of ganciclovir or FGCV with pure HSV1-TK enzyme. The solution was incubated at 37°C for 60 min and analyzed by HPLC.

HSV1-TK Enzyme Assay. Cell or liver extracts were incubated for 20 min with 8-[^{3}H]GCV to determine the formation of phosphorylated 8-[^{3}H]GCV. 8-[^{3}H]GCV is separated from phosphorylated 8-[^{3}H]GCV by using a DE-81 filter (Whatman) (22). To improve the accuracy of this assay as compared with our previous use of this assay (15), we used a control sample in which identical steps are used, except the filter is not washed (23). This unwashed sample measures total substrate (8-[^{3}H]GCV) available for phosphorylation and is used to normalize the activity retained on the washed filter. Results are reported as percent conversion of 8-[^{3}H]GCV in (dpm/μg protein per min of cell or tissue extract)/(dpm of control sample) $\times$ 100.

HSV1-tk Message Levels. Northern analyses were performed to determine the HSV1-tk mRNA levels from cells and murine liver extracts and normalized to glyceraldehyde-3-phosphate dehydrogenase mRNA levels (15).

Analysis of 8-[^{3}H]GCV and FGCV Metabolites in Cells. Cell extracts were obtained after either C6 or C6-stb-tk+ cells were incubated with 8-[^{3}H]GCV (1 μCi/ml) or FGCV (20 μCi/ml) for 15, 30, 60, 120, and 180 min. Cell pellets were treated with 50 μl 1.5 M perchloric acid ($HClO_4$) at 0°C for 30 min. The solutions were neutralized with 1 M KOH and centrifuged to remove the precipitate, and the supernatants were injected onto the HPLC column. Fractions (1 ml) were collected directly into scintillation vials, and radioactivity was determined. Alkaline hydrolysis of the acid-insoluble fraction was performed as follows: The pellet was dissolved in 100 μl of 1 M NaOH and incubated for 1.5 h at 37°C. Trichloroacetic acid (5%, 400 μl) was added and the solution was centrifuged at 10,000 rpm for 30 sec. The supernatant and a subsequent wash were treated with KOH, and the radioactivity was determined. The radioactivity in the alkali labile fraction (expressed as a percentage of the total radioactivity) represents the phosphorylated metabolite incorporated into RNA/DNA. The pellet was resuspended in dimethyl sulfoxide and counted for radioactivity.

Cell Uptake Studies. Uptake of 8-[^{3}H]GCV (0.76 μCi/ml, 1.5×10^{-5} mg/ml) and FGCV (3 μCi/ml, 2.1×10^{-4} mg/ml) was compared directly in C6 and C6-stb-tk+ cells. The higher concentration of FGCV is required because of the lower specific activity of FGCV relative to 8-[^{3}H]GCV. The cells were incubated at 37°C for 15, 30, 60, 120, and 240 min. At the end of each incubation period, radioactivity in the medium was measured. The wells were washed with cold PBS, the cells were harvested using a cell scraper, and the cell-associated radioactivity was determined. Triplicate samples were performed at each time point for all uptake studies. The same wells also were used for determining total protein content (24). Data are expressed as the net accumulation of probe in [dpm cells/(dpm of medium at start of exposure)/μg protein] $\pm$ SE].

Analysis of FGCV Metabolites in Liver, Blood, and Urine. Animal care and euthanasia were performed by using criteria approved by the University of California at Los Angeles Animal Research Committee. Samples of the mouse livers (left lobe) were removed to analyze samples for metabolites. Liver tissue was placed in perchloric acid (1.5 M, 500 μl/10 mg, vol/wt, precooled in ice) and homogenized for 1 min at 10,000 rpm in a Power Gen Model 125 Homogenizer (Fisher Scientific). After centrifugation at 5,000 rpm for 20 min at 4°C, the supernatant was neutralized with 1 M KOH. The pellet constituted the acid-insoluble fraction. The precipitate was removed by centrifugation and the supernatant was injected onto the HPLC column. HPLC analyses of urine and plasma samples obtained from mice at 180 min after FGCV injection also were performed. Blood was collected in heparinized tubes and centrifuged at 4°C at 3,000 rpm for 10 min. Plasma was decanted and deproteinized with 1.5 M $HClO_4$. The samples was centrifuged for 15 min at 4°C. A 50-μl sample was injected onto the HPLC column. For urine, the sample was deproteinized and centrifuged at 3,000 rpm for 10 min and a 20-μl sample was used for HPLC analysis.

PET Imaging of Mice. Mice were anesthetized with Avertin (5%, 150 mg/kg) before the injection of tracer, placed in a spread-supine position on a cardboard slat, and imaged using the microPET scanner with the long axis of the mouse parallel to the long axis of the scanner (7). Acquisition time was 64 min (8 min per bed position; eight bed positions), and images were reconstructed by using three-dimensional filtered back-projection, with an isotropic image resolution of 1.8 mm and a volumetric resolution of $\approx$8 mm^3. For dynamic imaging mice were imaged on an ACAT PET (CTI, Knoxville, TN) scanner and image analysis was performed as described previously (25).

Quantitation of Fluorine-18 Retention in Murine Livers by microPET Image Analysis. Regions of interest (ROI) were drawn over the left liver lobe image on decay-corrected whole-body coronal images. The counts per pixel/min obtained from the ROI were converted to counts per ml/min by using a calibration constant obtained from scanning a cylinder phantom in the microPET scanner. The ROI counts per ml/min were converted to counts per g/min, assuming a tissue density of 1 g/ml, and divided by the injected dose to obtain an image ROI-derived percent injected dose of FGCV retained per gram of liver (FGCV %ID/g liver).

Digital Whole-Body Autoradiography. Freezing, preparation of mouse whole-body coronal sections (45-μm thickness), and DWBA were performed as described previously (15), using a FUJI BAS 5000 Phosphorimager and digital plates with a resolution of $\approx$100 μm.

RESULTS

FGCV Is a Substrate for HSV1-TK *in Vitro*. Ganciclovir and its metabolites are well characterized by HPLC and NMR (26,

27). The ability of FGCV to serve as a substrate for HSV1-TK has not been reported previously. We first demonstrated that HSV1-TK can phosphorylate FGCV. Products produced when ganciclovir and FGCV are incubated with HSV1-TK have similar HPLC retention times. For both substrates, HPLC peaks are seen at ≈3 and ≈9 min (not shown). Under similar HPLC conditions, ganciclovir and ganciclovir monophosphate are reported to elute at ≈3 and ≈11 min (26).

The ≈9-min ganciclovir-derived peak corresponding to ganciclovir monophosphate could be reduced by treatment with alkaline phosphatase. Identical results are obtained with the peak presumably corresponding to the monophosphate form of FGCV. For both ganciclovir and FGCV, the ≈9-min HPLC peaks decreased and the ≈3-min HPLC peaks increased in response to alkaline phosphatase treatment, suggesting that the ≈9-min peaks correspond to ganciclovir monophosphate and FGCV monophosphate (not shown).

C6 Cells Expressing HSV1-tk Convert FGCV to the Phosphorylated Forms. C6-stb-tk+ cells have a 5-fold-greater level of HSV1-tk message and a 12-fold-greater level of HSV1-TK enzyme activity than control C6 cells (data not shown). The radioactive products derived from 8-[^{3}H]GCV or FGCV, after incubation with C6-stb-tk+ cells, have similar HPLC retention times, suggesting that ganciclovir and FGCV are converted to similar products in these cells. Three peaks at ≈9, ≈16, and ≈32 min were obtained with both 8-[^{3}H]GCV and FGCV, consistent with the mono-, di-, and triphosphate analogs. Previously published results with similar HPLC conditions report peaks at ≈11, ≈19, and ≈32 min for the mono-, di, and triphosphates, respectively, when using ganciclovir (26). For increasing incubation times, the peaks seen at ≈16 and ≈32 min increased, whereas the peak corresponding to ≈9 min decreased, consistent with cellular phosphorylation of ganciclovir monophosphate and FGCV monophosphate. In contrast, 8-[^{3}H]GCV or FGCV incubated with control C6 cells, followed by HPLC analysis of cell extracts, showed only a ≈3-min peak. Some radioactivity in the C6-stb-tk+ cell extract was associated with the cellular DNA/RNA fraction for both 8-[^{3}H]GCV (18 and 60% at 30 and 120 min, respectively) and FGCV (10 and 35% at 30 and 120 min, respectively). In contrast, less than 5% of the total radioactivity retained in cells was incorporated into DNA/RNA in C6 control cells with either substrate for incubation times of up to 120 min.

FGCV Accumulates in Cells that Express HSV1-tk. We first compared the accumulation of radioactivity in C6 and C6-stb-tk+ cells for both 8-[^{3}H]GCV and FGCV (Fig. 1). There is a significant difference ($P < 0.01$) in the accumulation for both substrates between the two cell lines for all time points ≥30 min. At 15 min, only 8-[^{3}H]GCV shows a significant difference ($P < 0.01$) in accumulation between the two cell lines. Greater accumulation for 8-[^{3}H]GCV, as compared with FGCV, occurs in the C6-stb-tk+ cells ($P < 0.01$, for all time points), even though a lower 8-[^{3}H]GCV concentration was used.

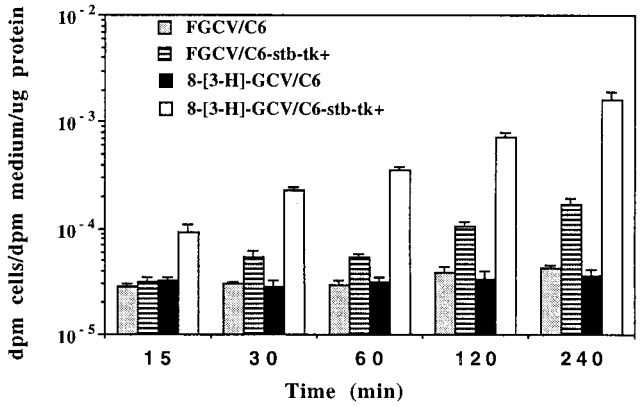

FIG. 1. 8-[^{3}H]GCV and FGCV accumulation in cells expressing HSV1-tk. C6 control cells and C6-stb-tk+ were incubated with either 8-[^{3}H]GCV or FGCV for up to 240 min. Results are for net accumulation of each tracer (log scale) in both cell types as a function of time. Bars represent SE based on triplicate determinations.

Next, accumulation of both 8-[^{3}H]GCV and FGCV was correlated with levels of adenovirus, HSV1-tk mRNA, and HSV1-TK enzyme in AdCMV-HSV1-tk-infected cells. C6 cells were seeded in seven t-75 flasks. Twenty-four hours later, 0.1, 0.5, 0.75, 1, 1.5, and 2×10^9 pfu/ml of AdCMV-HSV1-tk virus (to produce C6 tk+ cells) or 2×10^9 pfu/ml of control virus (to produce C6 tk− cells) were added to the flasks. For the AdCMV-HSV1-tk virus flasks, control virus also was added to maintain the total viral titer fixed at 2×10^9 pfu/ml. 8-[^{3}H]GCV (0.74 μCi/ml; 1.4×10^{-5} mg/ml) or FGCV (2 μCi/ml; 1.4×10^{-4} mg/ml) was incubated for 120 min with all cells, and accumulation was measured. C6 cell lines transfected with varying AdCMV-HSV1-tk levels demonstrate a good correlation between cellular accumulation of fluorine-18 radioactivity (range, 0.00006–0.0001 dpm cells/dpm medium per μg protein) and (*i*) number of virus plaque-forming units (pfu) added ($r^2 = 0.74$), (*ii*) HSV1-tk mRNA ($r^2 = 0.73$), and (*iii*) HSV1-TK enzyme ($r^2 = 0.80$). Similar results ($r^2 \sim 0.8$) were obtained with 8-[^{3}H]GCV, except that a larger dynamic range for accumulation of tritium radioactivity (range, 0.00005–0.001 dpm cells/dpm medium per μg protein) and steeper slopes were noted (data not shown).

In summary, *in vitro* and cell culture results demonstrated similar metabolites but lower accumulation and smaller dynamic range of accumulated radioactivity with FGCV as substrate as compared with 8-[^{3}H]GCV over equivalent levels of HSV1-TK. However, FGCV appears to be a good candidate to image HSV1-tk reporter gene expression *in vivo*.

FGCV Is Converted to Metabolic Products that Are Retained in Livers of Mice Expressing HSV1-tk. We next characterized the effectiveness of FGCV as a substrate for hepatic HSV1-TK *in vivo*. When mice are tail vein-injected with adenoviral vectors carrying reporter genes, expression is much greater in liver than in other tissues (15, 28). Swiss–Webster mice were injected by tail vein with 1.0×10^9 pfu of AdCMV-HSV1-tk or 1.0×10^9 pfu of control virus. Forty-eight hours later, animals received a tail vein injection of FGCV (80–130 μCi). Animals were sacrificed after 180 min. HPLC analysis of liver extracts from animals injected with control virus show that FGCV elutes with a retention time of ≈3 min. Greater than 94% of the total liver radioactivity was in the form of FGCV, with less than 5% associated with the DNA/RNA fraction. In mice injected with AdCMV-HSV1-tk virus, radioactivity is present in four major forms. The predominant peak at ≈16 min corresponding to a retention time similar to the diphosphate of ganciclovir presumably is the diphosphate of FGCV (Fig. 2). Furthermore, 30% of the radioactivity retained in the liver was associated with the DNA/RNA fraction. The retention times obtained from liver samples agree well with those obtained in cell culture for both FGCV and 8-[^{3}H]GCV and with those reported in the literature for ganciclovir (26). In summary, in C6 cells expressing the HSV1-tk reporter gene and in livers of mice expressing HSV1-tk, FGCV can be sequestered as a result of HSV1-tk gene expression.

FGCV Is Stable *in Vivo*. It is important that a PET reporter probe be stable in blood and peripheral tissues and not be degraded significantly to labeled metabolic forms with properties different from the original probe or to labeled forms that are retained in tissues in the absence of expression of the PET reporter gene (3). Ganciclovir is quite stable *in vivo* (29). FGCV is also quite stable *in vivo*. HPLC analysis of urine and plasma samples obtained from mice at 180 min after FGCV injection demonstrated that greater than 97% of the activity was in the form of the parent nucleoside.

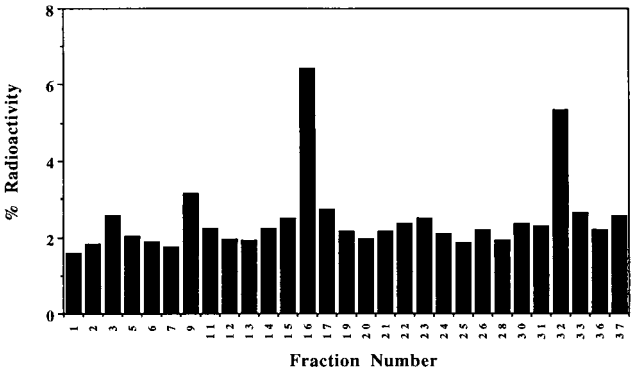

FIG. 2. FGCV metabolites present in livers of mice expressing HSV1-tk. A mouse was injected with 1.0×10^9 pfu of AdCMV-HSV1-tk virus followed by injection of FGCV 48 h later and sacrifice 180 min later. HPLC analysis of the liver sample shows peaks corresponding to ≈3, ≈9, ≈16, and ≈32 min, which likely represent FGCV, FGCV-monophosphate, FGCV-diphosphate, and FGCV-triphosphate, respectively. Thirty percent of the radioactivity retained in the liver was present in the DNA/RNA fraction (not shown).

Retention of FGCV Metabolites Can Be Used to Image HSV1-tk Reporter Gene Expression, both by DWBA and microPET. Two adult (10- to 12-week-old) Swiss–Webster mice (25–35 g) were studied by both microPET and DWBA imaging, using FGCV. One mouse was injected by tail vein with 1.5×10^9 pfu of control virus, and the other with 1.5×10^9 pfu of Ad-CMV-HSV1-tk virus. Forty-eight (±1) hours later FGCV (80–130 μCi) was injected by tail vein. The mice were imaged by microPET 2 h after FGCV injection. Immediately after microPET imaging, the animals were sacrificed and sections were analyzed by DWBA to directly compare microPET and DWBA images for FGCV biodistribution (Fig. 3). Minimal signal is observed in the liver of the mouse injected with control virus. In contrast, a good signal is present in the liver (relative to surrounding regions) of the mouse injected with AdCMV-HSV1-tk adenovirus. Activity is present in the urinary tract and the intestines of both mice because of elimination of FGCV by these routes. The combination of HSV1-tk as a PET reporter gene and FGCV as a positron-labeled PET reporter probe permits, in living animals, monitoring of HSV1-tk reporter gene expression.

Hepatic FGCV Retention Quantitatively Reflects HSV1-tk Reporter Gene Expression, and FGCV Kinetics Can Be Assessed with Dynamic PET Imaging. We next examined the relationship between the percentage of FGCV retained in liver after FGCV injection (%ID/g liver) and three other variables: (*i*) HSV1-tk mRNA expression, (*ii*) HSV1-TK enzyme activity, and (*iii*) concentration of injected virus. Fourteen adult Swiss–Webster mice were injected by tail vein with 0–2.0×10^9 pfu of AdCMV-HSV1-tk virus and additional control virus to maintain the total viral titer fixed at 2.0×10^9 pfu. Forty-eight (±1) hours later animals received a tail vein injection of FGCV (80–130 μCi). The probe was allowed to distribute for 180 ± 4 min before sacrificing the mouse. Radioactivity determinations in liver (left lobe) were normalized by the weight of the liver and amount of radioactivity injected to obtain FGCV %ID/g liver. Small samples of the left lobe of the liver (0.1–0.4 g each) also were used for the determination of HSV1-tk mRNA levels (normalized to glyceraldehyde-3-phosphate dehydrogenase) and HSV1-TK enzyme levels.

Correlation between hepatic HSV1-tk mRNA and HSV1-TK enzyme is very good ($r^2 = 0.81$) (Fig. 4*A*). A high positive correlation with hepatic retention of FGCV products (FGCV %ID/g liver) was observed for HSV1-tk mRNA levels (Fig. 4*B*) ($r^2 = 0.81$) and for HSV1-TK enzyme activity (Fig. 4*C*) ($r^2 = 0.71$). In contrast, correlation between levels of AdCMV-HSV1-tk virus injected and FGCV %ID/g liver were poor ($r^2 = 0.39$) (not shown). These latter data emphasize the need for a separate measurement to quantitate effective levels of virally mediated gene delivery in target tissues *in vivo*.

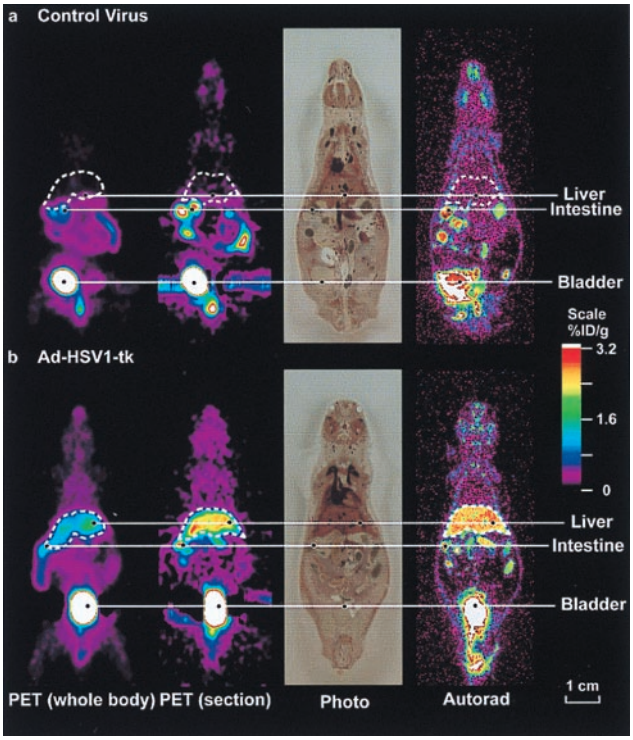

FIG. 3. MicroPET and DWBA images of mice after AdCMV-HSV1-tk and control virus administration. Swiss–Webster mice were injected via the tail vein with 1.5×10^9 pfu of control virus (*a*) or 1.5×10^9 pfu of AdCMV-HSV1-tk virus (*b*). For each mouse, a whole-body mean coronal projection image of the fluorine-18 activity distribution is displayed on the left. The liver outline, in white, was determined from both the FGCV signal and cryostat slices. The second images from the left are coronal sections, approximately 2-mm thick, from the microPET. After their PET scans, the mice were killed, frozen, and sectioned. The next images are photographs of the tissue sections (45-μm thickness) corresponding to approximately the midthickness of the microPET coronal section. The images on the right are DWBA of these tissue sections. The color scale represents the FGCV %ID/g. Images are displayed on the same quantitative color scale to allow signal intensity comparisons among them.

Although it is well established that ROI values from PET images accurately reflect (within the limits of resolution) tissue tracer counts (30), we used four mice to demonstrate that this relationship also is valid specifically for FGCV. For four of the mice studied for FGCV hepatic retention studies, imaging was performed 2 h after injection of FGCV, before sacrifice, on a microPET scanner. MicroPET images were analyzed for FGCV %ID/g liver by using ROI analysis. MicroPET-derived FGCV %ID/g liver, as determined from an ROI drawn over summed coronal images of the left liver lobe, did not differ significantly from those of FGCV %ID/g liver obtained by well counter ($P < 0.05$).

Dynamic PET Imaging of Mice Demonstrates FGCV Kinetics *in Vivo*. Two adult Swiss–Webster mice were injected by tail vein with 1.0×10^9 pfu of AdCMV-HSV1-tk virus and two were injected with 1.0×10^9 pfu of control virus. Forty-eight (±1) hours later dynamic imaging was performed in an ACAT scanner. Each animal received a tail vein injection of FGCV (80–130 μCi). Emission scanning was started within 30 sec from the time of FGCV injection.

The myocardial time–activity curves show a rapid decrease as a function of time, with less than 20% of peak activity remaining at 20 min (time–activity data not shown). The spillover-corrected liver time–activity curve from each mouse

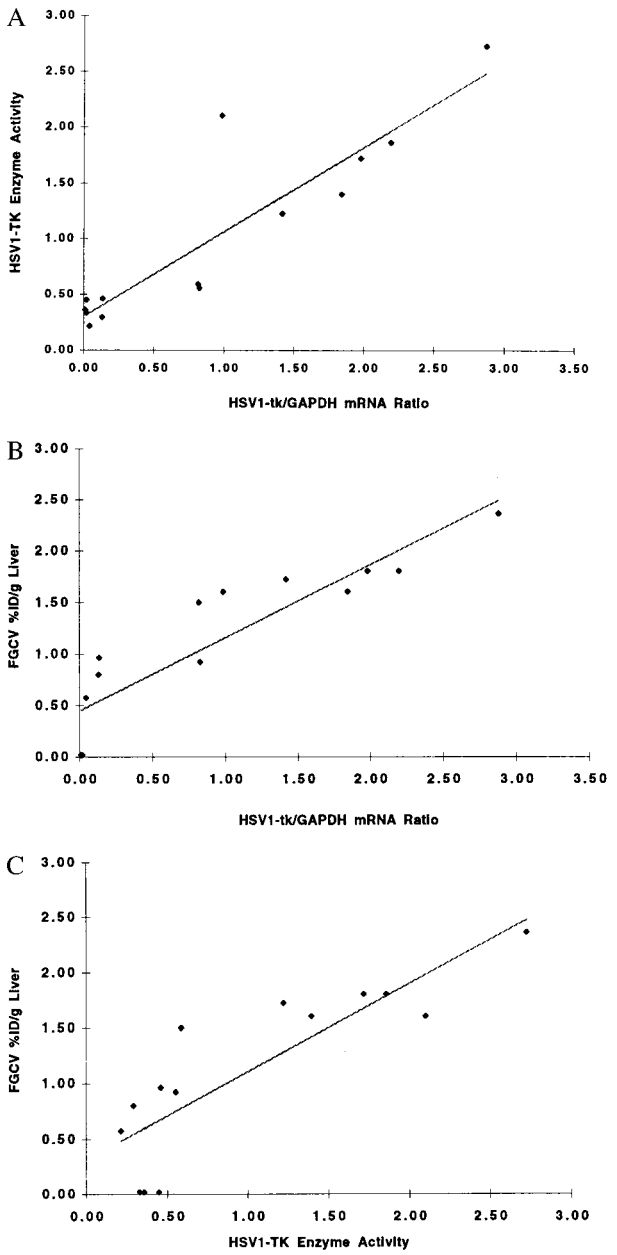

FIG. 4. FGCV retention in liver as a function of HSV1-tk gene expression. Fourteen adult Swiss–Webster mice were injected by tail vein with 0–2.0 $\times$ 10^9 pfu of AdCMV-HSV1-tk virus and additional control virus to maintain the total viral burden to be fixed to 2.0 $\times$ 10^9 pfu. Forty-eight ($\pm$1) hours later, animals received a tail vein injection of FGCV. Animals were sacrificed 180 min later. Livers were removed and liver samples were analyzed for (*i*) fluorine-18 retained in tissue, (*ii*) HSV1-tk mRNA levels normalized to glyceraldehyde-3-phosphate dehydrogenase, and (*iii*) HSV1-TK enzyme levels. (*A*) HSV1-TK enzyme levels vs. HSV1-tk mRNA levels ($y = 0.76x + 0.30$, $r^2 = 0.81$). (*B*) FGCV %ID/g liver vs. HSV1-tk mRNA levels ($y = 0.71x + 0.44$, $r^2 = 0.81$). (*C*) FGCV %ID/g liver vs. HSV1-TK enzyme activity ($y = 0.79x + 0.31$, $r^2 = 0.71$). Each point represents data from a different mouse.

injected with AdCMV-HSV1-tk shows rapid accumulation of activity, with >95% of the activity at 1 h achieved within 15 min. The spillover-corrected liver time–activity curve from each mouse injected with control virus does not show any significant accumulation of activity, as expected. Other organs, with the exception of the kidneys, intestines, and bladder, also show very rapid clearance of FGCV. Kinetics of FGCV demonstrate rapid targeting to HSV1-tk-positive tissues, with fast clearance from the blood, supporting the ability to rapidly assay HSV1-tk expression *in vivo*.

DISCUSSION

We have synthesized FGCV and demonstrated that it is a substrate for HSV1-TK. When FGCV is injected into mice we observe fluorine-18 retention in tissues expressing HSV1-tk. FGCV metabolites have similar HPLC retention times as ganciclovir metabolites, both in cells and in hepatic tissue expressing HSV1-tk. Fluorine-18 retention both in cells and in liver correlates well with HSV1-tk gene expression. Imaging of the HSV1-tk reporter gene in living mice produces a good image contrast between liver tissue expressing the HSV1-tk reporter gene and surrounding tissues with minimal or no reporter gene expression.

FGCV produces a lower %ID/g liver when compared with our previously reported results with 8-[^{14}C]GCV (15). Over a similar range of HSV1-tk expression, the range of %ID/g liver for 8-[^{14}C]GCV and FGCV is $\approx$0–23% and $\approx$0–3%, respectively. These results are consistent with the results of substrate conversion by HSV1-TK *in vitro*; higher concentrations of FGCV and longer incubation periods (as compared with 8-[^{3}H]GCV) result in lower levels of FGCV monophosphate production. The highly electronegative fluorine-18 in FGCV may cause decreased FGCV efficiency for docking in the HSV1-TK enzyme pocket, which is dependent on hydrogen bonding (31), leading to a lower V_{max}/K_m ratio for FGCV vs. ganciclovir. K_m and V_{max} analyses for FGCV as substrate for HSV1-TK currently are underway. Improvements in the choice of substrate (e.g., penciclovir) (32) and the use of mutant HSV1-TK enzymes with enhanced affinity for ganciclovir as substrate (33) may improve the sensitivity of HSV1-tk reporter gene detection, permitting imaging of lower levels of HSV1-tk reporter gene expression. There may be some plateauing of the FGCV %ID/g liver at higher levels of HSV1-tk expression, although the relatively high r^2 values obtained support a linear relationship. Tracer kinetic modeling of dynamic PET data may help to separate FGCV transport from phosphorylation, thereby improving the ability to quantitatively correlate image intensity with HSV1-TK levels (34).

The use of FGCV as a reporter probe to image gene expression mediated by HSV1-tk has attractive features, namely, the rapid *in vivo* clearance of FGCV, its negligible *in vivo* peripheral metabolism, and its high specificity for viral thymidine kinase. These features permit excellent signal-to-noise ratios for *in vivo* imaging in a relatively short period of 3 h. This feature is very convenient in applications in which repeated evaluation of gene expression (e.g., induction of expression by environmental stimuli in animal models) over short periods of time is needed. In contrast, reporter probes with substantial affinity for mammalian TK and, concomitantly, less specificity for HSV1-TK (e.g., FIAU labeled with iodine-124) seem to require 24–48 h between probe administration and tomographic analysis (9, 18). It will be of great interest to compare FIAU labeled with iodine-124 (18) and acycloguanosine derivatives labeled with fluorine-18 for their quantitative reflection of HSV1-tk expression, sensitivity, and ability to rapidly and repetitively image HSV1-tk expression by PET.

Ganciclovir has minimal toxicity when administered in human suicide gene therapy studies (350 mg i.v. twice daily) over a course of $\approx$2 weeks (35). The use of FGCV for imaging in humans is not expected to lead to significant cytotoxicity, because of the relatively low levels of FGCV administered (10-mCi dose would be $\approx$0.8 mg), the rapid clearance of tracer, and the lower accumulation of FGCV as compared with ganciclovir in target tissue.

When HSV1-tk is used as a reporter gene along with a second, therapeutic gene, it is possible that selective pressures

in vivo might differentially modulate expression of the HSV1-tk reporter gene and the therapeutic gene. To minimize such potential problems in gene therapy applications, we anticipate using vectors in which a single promoter drives both the PET reporter gene and the therapeutic gene as a bicistronic message, with an internal ribosomal entry site to facilitate translation of both proteins from a common message (5, 6). Furthermore, when HSV1-tk is used as a suicide gene, as is being done in several human cancer gene therapy trials (36), an alternate PET reporter gene may be used for monitoring HSV1-tk suicide gene expression. Alternatively, the HSV1-tk gene could be used both as a reporter and suicide gene, if imaging is performed when pharmacological levels of ganciclovir are relatively low, to prevent direct competition by ganciclovir for FGCV uptake and phosphorylation. In anticipation of applications requiring a second PET reporter gene, we have investigated in mice the use of the dopamine type 2 receptor PET reporter gene with 3-(2′-[18F]fluoroethyl)spiperone as a PET reporter probe (37).

Reporter genes also have been used in transgenic animals to analyze (*i*) the relationship between presumptive gene-specific, transcriptional-regulatory sequences and gene expression and (*ii*) effects of developmental and environmental perturbations on gene expression. In both contexts, analysis of reporter genes such as β-galactosidase and luciferase is limited to measurements at single times in tissue preparations from sacrificed animals. Using PET reporter genes and positron-labeled PET reporter probes in transgenic animals, it also will be possible to rapidly and repeatedly monitor, in the same animal, time-dependent developmental, environmental, and experimental influences on gene expression.

We thank W. Ladno, J. Edwards, D. J. Liu, A. Borghei, P. Shah, and R. Sumida for technical assistance. This study was supported by an interdisciplinary seed grant from the University of California at Los Angeles (UCLA)–Jonsson Cancer Center Foundation, the UCLA Gene Medicine Program, the University of California Biotechnology Grant, the Dana Foundation, and by Department of Energy Contract DEFC03–87ER60615.

1. Jacobs, W. R., Barletta, R. G., Udani, R., Chan, J., Kalkut, G., Sosne, G., Kieser, T., Sarkis, G. J., Hatfull, G. F. & Bloom, B. R. (1993) *Science* **260,** 819–822.
2. Misteli, T. & Spector, D. (1997) *Nat. Biotechnol.* **15,** 961–964.
3. Barrio, J. R. (1986) *Biochemical Principles in Radiopharmaceutical Design and Utilization* (Raven, New York).
4. Phelps, M. E. (1991) *Neurochem. Res.* **16,** 929–940.
5. Gambhir, S. S., Barrio, J. R., Herschman, H. R. & Phelps, M. E. (1999) *J. Nucl. Cardiol.*, in press.
6. Gambhir, S. S., Barrio, J. R., Herschman, H. R. & Phelps, M. E. (1999) *Nucl. Med. Biol*., in press.
7. Cherry, S. R., Shao, Y., Silverman, R. W., Meadors, K., Siegel, S., Chatziioannou, A., Young, J. W., Jones, W. F., Moyers, J. C., Newport, D., *et al.* (1997) *IEEE Trans. Nucl. Sci.* **44,** 1161–1166.
8. Tjuvajev, J. G., Stockhammer, G., Desai, R., Uehara, H., Watanabe, H., Gansbacher, B. & Blasberg, R. G. (1995) *Cancer Res.* **55,** 6126–6132.
9. Tjuvajev, J. G., Finn, R., Watanabe, K., Joshi, R., Oku, T., Kennedy, J., Beattie, B., Koutcher, J., Larson, S. & Blasberg, R. G. (1996) *Cancer Res.* **56,** 4087–4095.
10. Srinivasan, A., Gambhir, S. S., Green, L. A., Cherry, S. R., Sharfstein, S., Barrio, J. R., Satyamurthy, N., Namavari, M., Wu, L., Berk, A. J., *et al.* (1996) *J. Nucl. Med.* **37,** 107P (abstr.).
11. Alauddin, M. M., Conti, P. S., Mazza, S. M., Hamzeh, F. M. & Lever, J. R. (1996) *Nucl. Med. Biol.* **23,** 787–792.
12. Morin, K. W., Atrazheva, E. D., Knaus, E. E. & Wiebe, L. I. (1997) *J. Med. Chem.* **40,** 2184–2190.
13. Monclus, M., Luxen, A., Cool, V., Damhaut, P., Velu, T. & Goldman, S. (1997) *Bioorg. Med. Chem. Lett.* **7,** 1879–1882.
14. Haberkorn, U., Altmann, A., Morr, I., Knopf, K.-W., Germann, C., Haeckel, R. & Oberdorfer, F. (1997) *J. Nucl. Med.* **38,** 287–294.
15. Gambhir, S. S., Barrio, J., Wu, L., Iyer, M., Namavari, M., Satyamurthy, N., Bauer, E., Parrish, C., MacLaren, D., Borghei, A., *et al.* (1998) *J. Nucl. Med.* **39,** 2003–2011.
16. De Winter, H. & Herdewijn, P. (1996) *J. Med. Chem.* **39,** 4727–4737.
17. Elion, G. B. (1993) *J. Med. Virol.* Suppl. 1, 2–6.
18. Tjuvajev, J. G., Avril, N., Oku, T., Sasajima, T., Miyagawa, T., Joshi, R., Safer, M., Beattie, B., DiResta, G., Daghighian, F., *et al.* (1998) *Cancer Res.* **58,** 4333–4341.
19. Barrio, J. B., Namavari, M., Phelps, M. E. & Satyamurthy, N. (1996) *J. Org. Chem.* **61,** 6084–6085.
20. Barrio, J. R., Namavari, M., Srinivasan, A., Gambhir, S., Cherry, S., Herschman, H., Phelps, M. E. & Satyamurthy, N. (1997) in *XII International Symposium on Radiopharmaceutical Chemistry* (Uppsala, Sweden), 348 pp.
21. Barrio, J. R., Namavari, M., Satyamurthy, N., Srinivasan, A., Herschman, H. & Gambhir, S. (1996) *J. Nucl. Med.* **37,** 193P (abstr.).
22. Hruby, D. E. & Ball, L. A. (1981) *Virology* **113,** 594–601.
23. Furlong, N. B. (1963) *Anal. Biochem.* **5,** 515–522.
24. Bradford, M. M. (1976) *Anal. Biochem.* **72,** 248–254.
25. Green, L. A., Gambhir, S. S., Srinivasan, A., Banerjee, P. K., Hoh, C., Cherry, S., Sharfstein, S., Barrio, J., Herschman, H. & Phelps, M. E. (1998) *J. Nucl. Med.* **39,** 729–734.
26. Smee, D. F., Boehme, R., Chernow, M., Binko, B. P. & Matthews, T. R. (1985) *Biochem. Pharmacol.* **34,** 1049–1056.
27. Birnbaum, K. B., Stolarski, R. & Shugar, D. (1994) *Biochim. Biophys. Acta* **1200,** 55–63.
28. Herz, J. & Gerard, R. D. (1993) *Proc. Natl. Acad. Sci. USA* **90,** 2812–2816.
29. Faulds, D. & Heel, R. C. (1990) *Drugs* **39,** 597–638.
30. Hoffman, E. J., Huang, S. C. & Phelps, M. E. (1979) *J. Comput. Assist. Tomogr.* **3,** 299–308.
31. Brown, D. G., Visse, R., Sandhu, G., Davies, A., Rizkallah, P. J., Melitz, C., Summers, W. C. & Sanderson, M. R. (1995) *Nat. Struct. Biol.* **2,** 876–881.
32. Bacon, T. H., Howard, B. A., Lindsay, C. S. & Malcolm, R. B. (1996) *J. Antimicrob. Chemother.* **37,** 303–313.
33. Black, M. E., Newcomb, T. G., Wilson, H.-M. P. & Loeb, L. A. (1996) *Proc. Natl. Acad. Sci. USA* **93,** 3525–3529.
34. Green, L. A., Gambhir, S. S., Barrio, J. R., Bauer, E., Nguyen, K., Namavari, M., Cherry, S. R., Herschman, H. & Phelps, M. E. (1998) *J. Nucl. Med.* **39,** Suppl., 10P (abstr.).
35. Sterman, D. H., Treat, J., Litzky, L. A., Amin, K. M., Coonrod, L., Molnar-Kimber, K., Recio, A., Knox, L., Wilson, J. M., Albelda, S. M. & Kaiser, L. R. (1998) *Hum. Gene Ther.* **9,** 1083–1092.
36. Blomer, U., Naldine, L., Verma, I. M., Trono, D. & Gage, F. H. (1996) *Hum. Mol. Genet.* **5,** 1397–1404.
37. MacLaren, D. C., Gambhir, S. S., Satyamurthy, N., Barrio, J. R., Sharfstein, S., Toyokuni, T., Wu, L., Berk, A. J., Cherry, S. R., Phelps, M. E. & Herschman, H. R. (1999) *Gene Therapy*, in press.